Earthquake Geotechnical Engineering for Protection and Development of Environment and Constructions – Silvestri & Moraci (Eds)
© 2019 Associazione Geotecnica Italiana, Rome, Italy, ISBN 978-0-367-14328-2

On the comparison of 3D, 2D, and 1D numerical approaches to predict seismic site amplification: The case of Norcia basin during the M6.5 2016 October 30 earthquake

A.G. Özcebe
University of Pavia, and Politecnico di Milano, Italy

C. Smerzini, R. Paolucci, H. Pourshayegan & R. Rodríguez Plata
Politecnico di Milano, Italy

C.G. Lai & E. Zuccolo
University of Pavia, Italy

F. Bozzoni
EUCENTRE, Pavia, Italy

M. Villani
ARUP, London, UK

ABSTRACT: This paper contains 3D/2D/1D ground response analyses of Norcia basin during the M6.5 2016 October 30 event by comparing the recorded response at NOR and NRC stations, which are located in mid-basin and near-fault conditions. Results show that 3D simulations may capture the overall response reasonably well, yet the simplification of vertical incidence seems to bias the results due to the presence of complex near-fault seismic wave propagation effects.

1 INTRODUCTION

1.1 *Definition of the research*

Standard engineering tools for the evaluation of local site amplification effects rely typically on one-dimensional numerical approaches under the assumption of horizontally layered soil structure and vertical propagation of seismic waves. Nevertheless, such approaches may not be apt to describe accurately the seismic amplification effects occurring in alluvial basins, as they cannot account for the complex morphology of the basin and its coupling with fault rupture propagation phenomena, as it has already been shown for the response of Gubbio basin during M6.0 September 26, 1997 Umbria-Marche event (Smerzini et al., 2011).

In this work, the ground motion recordings obtained in the epicentral area of the M6.5 2016 October 30 earthquake in Central Italy provides a meaningful observational dataset to verify the accuracy of different numerical approaches, 3D vs 2D vs 1D, for prediction of near-fault ground motion in alluvial basins. In order to carry out such a task, first the simulated ground motions are calculated using the spectral element code SPEED (Mazzieri et al., 2013) and then enrich the frequency content through ANN2BB approach (Paolucci et al., 2018). Subsequently, a rep-resentative rock motion obtained by the numerical simulations is propagated in 2D domain using FLAC2D (Itasca, 2016) solver and 1D domain using STRATA (Kottke and Rathje, 2010) code. It should be noted that all models share the same hysteretic model in terms of modulus degradation-strain relation (modulus degradation relation adopted

is presented in Figure 3). Details regarding the numerical models are presented from Section 2 to 4. Comparison of the results, on the other hand, are presented in Section 5.

All the analyses require the definition of the geotechnical model of Norcia basin and the bed-rock. Due to this reason, a brief representation of the modelled basin is presented in Section 1.2.

1.2 *Norcia basin model*

3D depth-velocity model of Norcia basin is constructed by assembling 9 cross-sections obtained through geological and geophysical methods (i.e. 2 seismic reflection sections from Böhm et al., 2011; 5 gravimetric profiles from Aringoli et al., 2014; 2 geologic sections from Motti, 2017), 83 H/V tests at various locations (i.e. 48 from Angeletti et al., 2018; 20 from Porreca et al., 2018; 15 from Bindi et al., 2011), 42 Vs-depth profiles (i.e. 39 from Angeletti et al., 2018; 2 from INGV-Milano; 1 from Bindi et al., 2011), 3 VP-depth profiles (i.e. 2 from Angeletti et al., 2018; 1 from Bindi *et al.,* 2011), 3 boreholes associated with SPT measurements (i.e. all from Angeletti *et al.,* 2018), and 4 boreholes associated with geotechnical laboratory tests (i.e. all from Venanti *et al.,* 2018). After the proper harmonization of the data, a single idealized VS-depth model is generated for whole basin and by using the idealized VS-depth relation, 3D sediment thickness model is generated by making use of the spatial interpolation schemes of MATLAB 2016b. Resulting mathematical model of Norcia basin is presented in Figure 1, which is also shared in the companion paper of this conference (Rodriguez-Plata *et al.,* 2018). In order to carry out 2D and 1D analyses, a profile that passes through seismic stations is selected as shown in Figure 2.

Material nonlinearity of the basin material is taken into account by fitting a modulus degradation and damping curves to the available resonant column data.

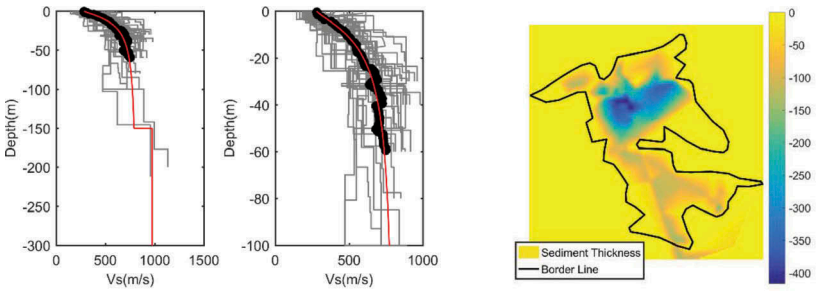

Figure 1. Idealized mathematical model of Norcia basin. Left: Shear-wave velocity (in m/s)-depth (in m) relation. Right: sediment elevation from ground surface (in m)

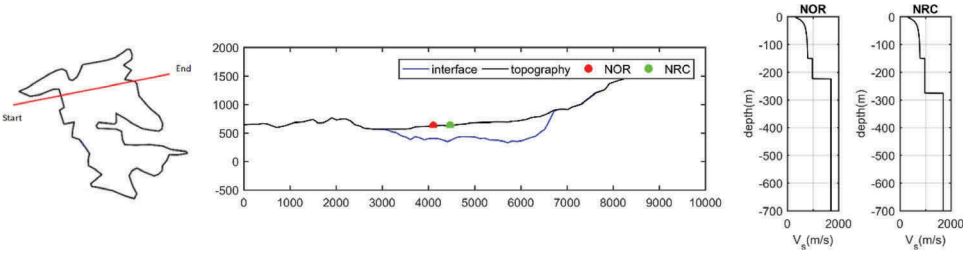

Figure 2. Left: Extracted section that crosses the northern Norcia basin and passes nearby two seismic stations (NOR and NRC). Center: Combined topography and depth of basin for the extracted section. Right: VS-depth plots for NRC and NOR. All length units are in meters.

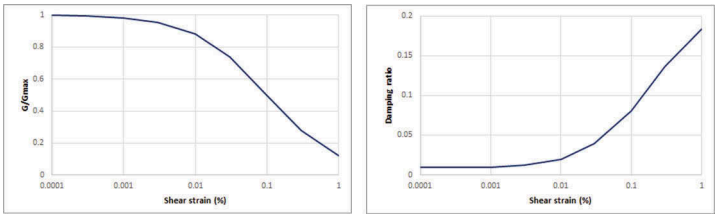

Figure 3. Secant shear modulus degradation (left) and damping ratio (right) curves.

2 3-D NUMERICAL MODELLING

2.1 *Definition of parameters*

In addition to the geotechnical setting defined in Section 1.2, the other key ingredients in constructing the 3D numerical model are (i) the definition of the kinematic slip distribution along the causative fault and (ii) the definition of the crustal velocity model.

Considering point (i), three published fault inversion studies (i.e. Chiaraluce *et al.,* 2017; Liu *et al.,* 2017; Pizzi *et al.,* 2018) are compared through preliminary analyses using the analytical method proposed by Hisada and Bielak (2003), based on the asymptotic integration of dynamic Green's functions in a linear viscoelastic layered half-space. It is found that the best agreement between the observations and simulations is obtained through the choice of the source slip distribution model proposed by Pizzi *et al.* (2018), together with the corresponding hypocentral location and fault geometry. The remaining parameters are calibrated through series of sensitivity analyses carried out using the codes of SPEED and Hisada. The final parameters are assigned as: V_{rup} = 1700 m/s (rupture velocity), τ=0.7 s with randomization (rise time), epicentral position = 42.84°N, 13.11°E, hypocentral depth = 7.0 km, fault length = 36 km, fault width = 13 km, depth to top of the fault = 1.8 km. Distributions of slip (S), rupture time (fc), and rise time (x) are presented in Figure 4.

Considering point (ii), the crustal 1-D structure used by Evangelista *et al.* (2017) for the L'Aquila region was considered. This model is very similar to that of Pizzi *et al.* (2017). Furthermore, preliminary analysis with Hisada code showed consistent waveforms at strong ground motion locations when a more complex crustal model, as proposed by Hermann *et al.* (2011), was adopted.

As the final step, surface topography and basin models are constructed. Large scale spectral element model (40 km x 50 km x 21 km) consisted of more than 350,000 elements of 3rd order, being able to propagate seismic waves up to a maximum frequency of 1.5 Hz.

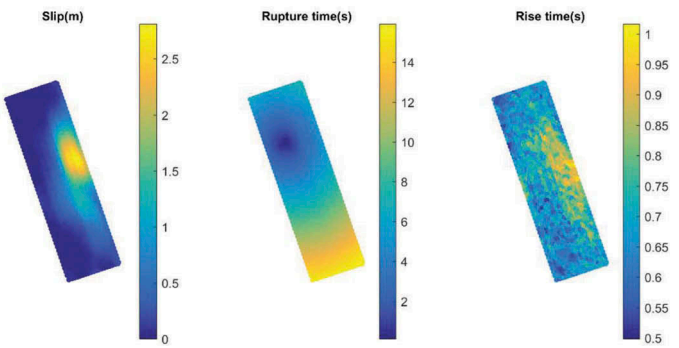

Figure 4. Distributions of slip (left), rupture time (center), and rise time (right) distributions considered in 3D ground response analyses carried out by SPEED code

It should be noted that two final 3D models are analyzed, that include and exclude the presence of the basin, in order to evaluate the impact of 3D basin effects on the results. Basin model uses the shear wave velocity profile shown in Figure 1 and nonlinear viscoelastic response based on the material curves presented in Figure 3.

2.2 *Frequency enrichment according to ANN2BB procedure*

Even in the presence of an ideal seismic source model that could generate reliable waveforms under a broadband frequency range, the accuracy of physics-based simulations (PBS) is limited to 1-1.5 Hz, owing to the increased computational burden with a finer mesh. Thus, typically, broad-band (BB) waveforms are generated by a hybrid approach which combines the low-frequency results from PBS with the high frequency results generated through stochastic approaches, by gluing the low-frequency and high-frequency portions of the spectrum with amplitude and phase matching algorithms. In this work, a method that makes use of Artificial Neural Networks (ANN) is considered, trained on a set of strong ground motions. The main idea behind this approach is, first, to train an ANN on a strong ground motion dataset (this case it is SIM-BAD by Smerzini *et al.,* 2014), in order to correlate the short-period (T<T*) spectral ordinates with the long period ones (T>=T*, T* being the threshold period beyond which the results of PBS are considered to be accurate), and, second, to use the trained ANN for estimating the short period response spectral ordinates for T<T*, using as the input the long period ones obtained by PBS. An example application on the response of NOR site is shown in Figure 5.

2.3 *Goodness of fit calculations and PGV maps*

In Figure 6, peak ground velocity (PGV) maps of the high frequency enriched 3D simulation results are presented in comparison with the values recorded at seismic stations. It can be observed that the spatial distribution and the agreement of PGV are reasonable.

In Figure 7, results of goodness of fit (GoF), according to Anderson (2004), point out good agreement of almost all parameters in three components. Especially in terms of the peak demand values (PGA, PGV), good to excellent conformity between the simulated and the recorded signals are evident. Nonetheless, the poor conformity in terms of cross correlation is also noticeable.

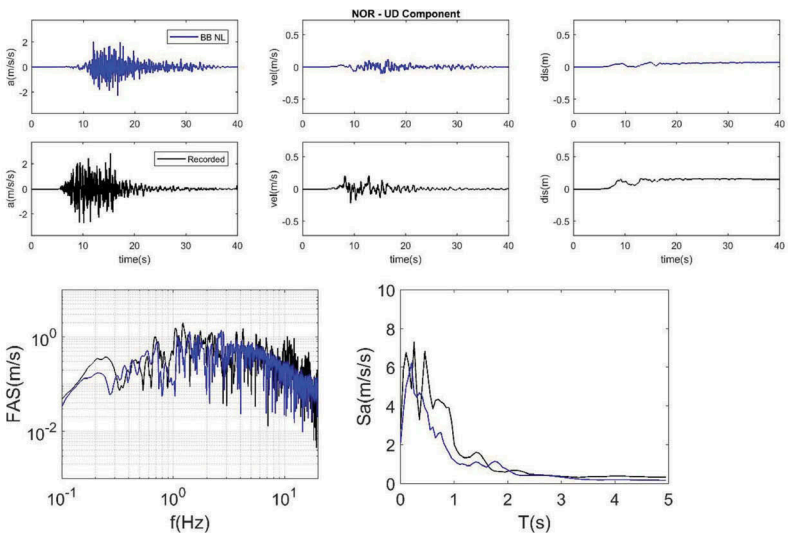

Figure 5. application of ANN2BB procedure on the simulated response of vertical component at NOR

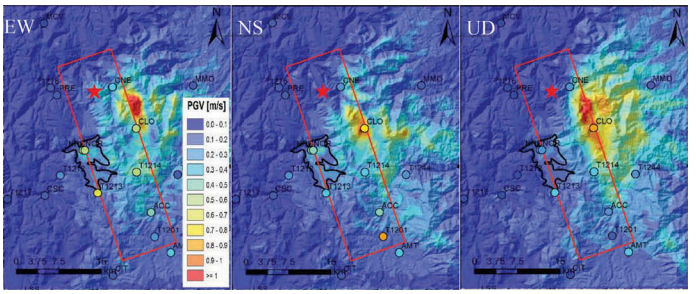

Figure 6. Peak ground velocity (PGV) maps obtained from 3D simulations after the enrichment of the high frequency content, in comparison with the values observed at stations. Left: EW (East-West) component, Center: NS (North-South) component, Right: UD (vertical) component (to be replaced with correct hypocenter)

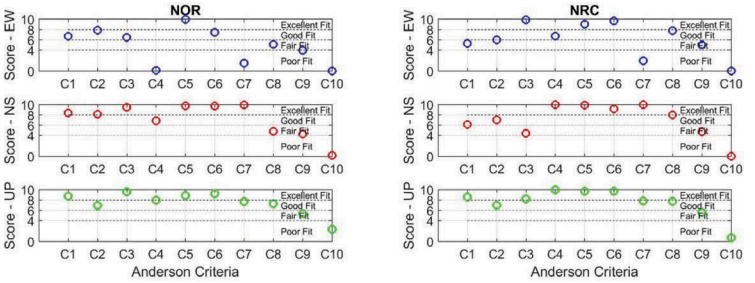

Figure 7. Goodness of fit scores (according to Anderson, 2004) of the three components of ground motion simulated at NOR (left) and NRC (right) stations (top row: EW, middle row: NS, bottom row: UP). C1: Arias Duration, C2: Energy Duration, C3: Arias Intensity, C4: Energy Integral, C5: PGA, C6: PGV, C7: SD (spectral displacements), C8: SA (spectral accelerations), C9: Fourier Spectra, C10: Cross-correlation.

3 2-D AND 1-D NUMERICAL MODELLING

3.1 *2-D numerical modelling*

For the section shown in Figure 2, 2-D model is created by using FLAC^{2D} v8. As shown in Figure 8, the modelled section has large scale dimensions (~1-2 km × 9 km) and accurate up to 6-7 Hz. The model has free-field dynamic boundaries (Cundall, 1980) at sides and absorbent boundary conditions (Lysmer and Kuhlemeyer, 1969) at bottom. The model contains the shear wave velocity depth relation presented in Figure 1 for the basin material, whereas the bedrock has Vs=1700 m/s as the first crustal layer. A hysteretic model respecting the modulus degradation curve presented in Figure 3 is adopted, damping is not controlled as it is taken into account automatically through unloading-reloading loops.

3.2 *1-D numerical modelling*

1-D models of NOR and NRC stations are created by using an equivalent-linear code: STRATA. Shear wave velocity-depth model of the extracted profiles are presented in Figure 2. Models use modulus degradation and damping curves stated in Figure 3.

3.3 *Broadband rock outcrop input motions used in 2D and 1D analyses*

Vertical propagations of plane S-waves in 2D and 1D simulations are modelled considering the broadband, outcrop motion at NRC component computed through 3D simulations,

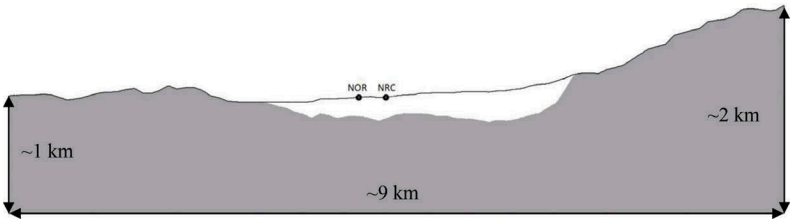

Figure 8. Dimensions of 2D finite difference model of the section presented in Figure 2.

without the presence of the basin (i.e. basin model is removed, and computation is made by using the crustal model only). Then, computed EW and NS components are rotated and combined properly to have the response parallel to the section shown in Figure 2.

In 2D simulations, input motion is provided as 1D stress-wave front ($\tau = \rho_r V_{s,r} \dot{u}$ in which p_r=2.5 t/m^3, $V_{s,r} = 1700 m/s$, $\dot{u}$: velocity-time response of rock motion) whereas in 1D analyses it is applied as rock-outcrop acceleration. Temporal representations of velocity and acceleration histories are provided in Figure 9.

4 COMPARISON OF RESPONSES AT SEISMIC STATIONS NRC AND NOR

In Figures 10 and 11, the records at NOR and NRC stations along the rotated components parallel to the 2D profile shown in Figure 2 are shown together with the results of 3D/2D/1D simulations.

Reasonably good agreement is observed at both stations (being better in NRC than in NOR), considering the epistemic uncertainties related to both the kinematic slip distribution model along the fault and to the 3D geologic model and the corresponding dynamic properties of the ground materials. Instead, when one compares the 1D and 2D response, it can be observed that those two models are comparable at both NOR and NRC stations, as expected because both stations are located at mid-basin. Minor differences are resulting from the fact that 2D model is accurate up to 7 Hz (thus Rayleigh damping is adjusted to damp out high frequencies), whereas 1D model has no such limitation.

When one compares the 3D simulation results with 1D and 2D, it is seen that the 3D response is more similar to the recorded one, both in amplitude and frequency content, because it accounts for surface waves contributions as well as non-perpendicular body wave propagation. As a matter of fact, from this point of view, the response of Norcia basin during M6.5 October 30, 2016 event is well in line with the response of Gubbio basin during M6.0 September 26, 1997 Umbria-Marche event, as published in Smerzini et al. (2011).

5 CONCLUSIONS

This paper presented 3D/2D/1D numerical modelling of strong ground motion stations on Norcia Basin during the event of M6.5 October 30, 2016. Indicators such as goodness of fit

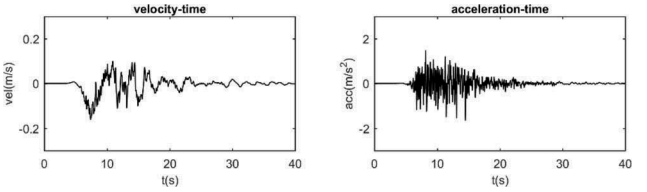

Figure 9. Input motions used in 2D and 1D analyses. Left: Velocity-time, right: acceleration-time

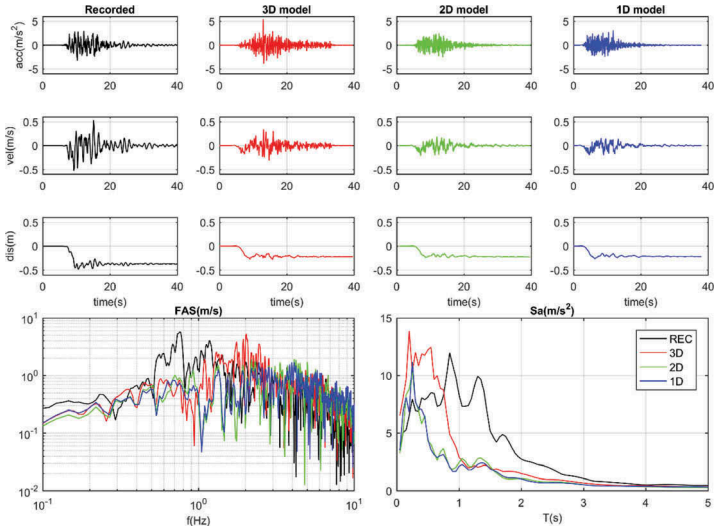

Figure 10. Recorded and simulated response at NOR station parallel to profile provided in Figure 2.

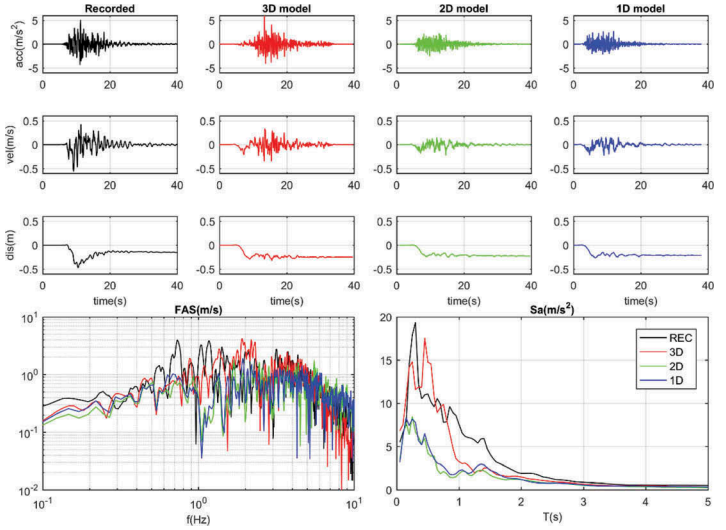

Figure 11. Recorded and simulated response at NRC station parallel to profile presented in Figure 2.

and distribution of PGV showed that 3D simulations could capture reasonably well the overall response registered in the surrounding stations. It is discussed that under near-field conditions, due to the strong presence of non-vertical incidence angles, conventional evaluation of basin effects in terms of aggravation factors depending solely on the geometry of the basin may become insufficient to explain the complex wave propagation phenomenon.

ACKNOWLEDGEMENTS

This work is co-financed by swissnuclear under the framework of SIGMA2 project and RELU-IS under the framework of Research Project RS2. Authors would like to acknowledge

the fruitful discussions made with Prof. Massimiliano Porreca from University of Perugia and Dr. Maurizio Vassallo, Dr. Francesca Pacor, and Dr. Lucia Luzi from INGV during the definition of the model for Norcia Basin. Furthermore, authors would like to express their gratitude to local geologists for their kind cooperation in sharing their data. Finally, Dr. Böhm's kind sharing of the reflection test data in digital format is warmly acknowledged.

REFERENCES

Anderson J.G. (2004). Quantitative measure of the goodness-of-fit of synthetic seismograms. *In* 13th World Conference on Earthquake Engineering Conference Proceedings, Vancouver, Canada.

Angeletti *et al.* (2018). Personal communications and digital data.

Aringoli D., Cavitolo P., Farabollini *et al.* (2014). Morphotectonic characterization of the quarternary intermontane basins of the Umbria-Marche Apennines (Italy). Rend. Fis. Acc. Lincei 25 (S2): 111–128.

Bindi D., Luzi L., Parolai S., Di Giacomo D., Monachesi G. (2011). Site effects observed in alluvial basins: the case of Norcia (Central Italy). Bulletin of Earthquake Engineering 9(6): 1941–1959.

Böhm G., Luzi L., Galadini F (2011). Tomographic depth velocity model below the plain of Norcia (Italy) for site effect studies. Bollettino di Geofisica Teorica ed Applicata 52(2).

Chiaraluce L., Di Stefano R., Tinti E., *et al.* (2017). The 2016 central Italy seismic sequence: a first look at the mainshocks, aftershocks, and source models. Seismological Research Letters 88(3): 757–771.

Cundall P.A., Hansteen S., Lacasse S., Selnes P.B. (1980). NESSI-Soil structure interaction program for dynamic and static problems. Norwegian Geotechnical Institute, Report 51508-09.

Evangelista L., del Gaudio S., Smerzini C. et al. (2017). Physics-based seismic input for engineering applications: a case study in the Aterno River valley, Central Italy. Bulletin of Earthquake Engineering 15(7): 2645–2671.

Herrmann R.B., Malagnini L., Munafò I. (2011). Regional moment tensors of the 2009 L'Aquila earthquake sequence. Bulletin of the Seismological Society of America 101(3): 975–993.

Hisada Y., Bielak J. (2003). A theoretical model for computing near-fault ground motions in layered half-spaces considering static offset due to surface faulting, with a physical interpretation of ling step and rupture directivity. Bulletin of Seismological Society of America 93(3): 1154–1168.

Itasca Consulting Group Inc. (2016). FLAC: Fast Lagrangian Analysis of Continua, Version 8. Computer code and User's Guide. Itasca Consulting Group Inc., Trasher Square East 708.

Kottke A.R., Rathje E.M. (2010). STRATA.

Liu C., Zheng Y., Xie Z., Xiong X. (2017). Rupture features of the 2016 Mw 6.2 Norcia earthquake and its possible relationship with strong seismic hazards. Geophysical Research Letters 44: 1320–1328.

Lysmer J., Kuhlemeyer R.L. (1969). Finite dynamic model for infinite media. Journal of Engineering Mechanics 95 (EM4): 859–877.

Mazzieri I., Stupazzini M., Guidotti R., Smerzini C. (2013). SPEED: Spectral Elements in Elastodynamics with Discontinuous Galerkin: a non-conforming approach for 3D multi-scale problems. International Journal for Numerical Methods in Engineering 95(12): 991–1010.

MATLAB (2016b). The MathWorks Inc., Natick, Massachusetts (USA).

Porreca M., Vasallo M. (2018). Personal communications and digital data.

Motti (2017). Personal comunications and data.

Pizzi A., Di Domenica A., Gallovič F. *et al.* (2017). Fault segmentation as constraint to be occurrence of the main shocks of the 2016 Central Italy seismic sequence. Tectonics 36(11): 2370–2387.

Venanti L.D. *et al.* (2018). Personal communications and digital data.

Paolucci R., Gatti F., Infantino M., *et al.* (2018). Broadband ground motions from 3D physics-based numerical simulations using artificial neural networks. Bulletin of the Seismological Society of America 108(3A): 1272–1286.

Rodriguez-Plata R., Smerzini C., Lai C.G., *et al.* (2018). A comparative study on time domain 1D/2D seismic ground response analysis of Norcia basin during the M6.5 2016 October 30 earthquake, 7ICEGE *(submitted paper)*.

Smerzini C., Paolucci R., Stupazzini M. (2011). Comparison of 3D, 2D and 1D numerical approaches to predict long period earthquake ground motion in the Gubbio plain, Central Italy. Bulletin of Earthquake Engineering 9:2007–2029.

Smerzini C, Galasso C, Iervolino I, Paolucci R (2014) Ground motion record selection based on broadband spectral compatibility, Earthquake Spectra, Vol. 30, No. 4, pp.1427–1448.